

## The influence of heating and cooling on the precision and microstructure of 3D printing results with PLA+ material

Dikky Antonius and Steven Austin Tondang\*

Jurusan Teknik Mesin, Universitas Kristen Indonesia, Jakarta, 13630, Indonesia

\*Corresponding author: steventondang04@gmail.com

### Abstract

The objective of this research is to investigate the influence of heating and cooling parameters on the accuracy and microstructure of 3D-printed products. Experimental methods were conducted by varying the heating and cooling parameters using PLA+ as the material. The results demonstrate that the heating and cooling parameters of the printing process significantly affect the precision and microstructure of 3D printed objects. Specimen printing was carried out using Ultimaker Cura 5.1.0 with a 100% infill density. Printing temperatures were set between 200°C and 240°C, with two variations of fan speeds at 80 mm/s and 100 mm/s. Other process parameters were kept constant, including a build plate temperature of 60°C, a grid infill pattern, and a printing speed of 50 mm/s. Three specimens were printed for each combination of fan speed and printing temperature. The printed specimens were measured using calipers, and then subjected to heating and cooling at different room temperatures before being measured again. The smallest average deviation was observed at a nozzle temperature of 240°C with fan speeds of 80% and 100%, specifically in specimens B-09 (with a bolt height of 17.60 mm, head diameter of 12.70 mm, bolt shaft diameter of 6.40 mm, and head thickness of 4.80 mm) and B-10 (with a bolt height of 17.60 mm, head diameter of 12.80 mm, bolt shaft diameter of 6.40 mm, and head thickness of 4.80 mm). Meanwhile, the microstructure analysis revealed that excessively high temperatures during the process could lead to increased deviations due to a structure resembling melting.

### Keywords:

Nozzle temperature, fan speed, 3D Printing, infill, PLA+.

### 1 Introduction

The emergence of 3D printing technology in the manufacturing sector has brought about significant changes globally. This technology, also known as additive manufacturing, has been in existence since the 1980s. 3D printing represents a revolutionary advancement in technology, gaining widespread popularity in academia and industry [1]. It holds immense potential in today's manufacturing industry, with Fused Deposition Modeling (FDM) being one of the most popular and affordable 3D printing methods [2,10,13]. Rapid prototyping is a process that utilizes 3D printing technology or other efficient methods to produce physical prototypes, significantly reducing the time required compared to traditional methods like mold making or manual shaping [3].

When it comes to printing materials, Polylactic Acid (PLA) stands out as the most commonly used filament in 3D printing [4].

PLA is a thermoplastic polymer material widely employed for creating 3D models [5, 8, 11]. Derived from biodegradable sources such as corn, tapioca, or sugarcane, PLA is considered environmentally friendly due to its biodegradability. It is capable of producing strong and aesthetically pleasing prints [6, 9, 12]. Scanning Electron Microscope (SEM) is an electron microscope designed specifically for direct observation of solid surfaces. Operating at magnifications ranging from 10 to 3,000,000 times, with a depth of field between 4 and 0.4 mm and a resolution of 1 to 10 nm, SEM is widely utilized in research and industrial applications due to its ability to provide compositional and crystallographic information. SEM focuses an electron beam on the surface of an object and captures images by detecting emitted electrons from the substance's surface [7].

This research aims to compare and analyze the effects of printing temperature and fan speed on the precision of printed specimens, as well as examine the microstructure of these specimens.

### 2 Research Methods

The method used in this research is the experimental method. The experimental steps are:

1. Creating the specimen model: the specimen model is designed using Onshape software as the design medium.
2. Converting the design: the design is then converted using Ultimaker Cura 5.1.0. This conversion is done to simulate the process that will occur when the parameters are set on the machine [18, 19, 22] and to change the file format of the design so that it can be read by the 3D printer that will be used.
3. Printing process: the printing process is carried out based on the process parameters that will be tested.
4. Measurement of dimensions after printing [16], each dimension of the specimen is measured using calipers. The specimen is then cooled to 31°C and measured again, then cooled again to 33°C and measured, and finally cooled to 22°C and measured once more.
5. SEM testing: the microstructure and surface roughness of each specimen are examined using Scanning Electron Microscopy (SEM).

#### 2.1 Sample

The sample dimensions are in the shape of a bolt, with sizes as shown in Fig. 1 and Table 1.

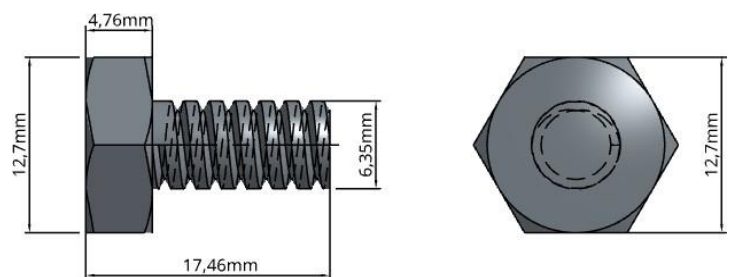


Fig. 1. Printed specimen.

Table 1. Actual specimen size

Bolt height (mm)	Head diameter (mm)	Shaft diameter (mm)	Head thickness (mm)
17.46	12.70	6.35	4.76

The sample was made using PLA+ [14, 15, 17] material with a melting point of 190°C to 240°C and a diameter of 1.75 mm. The design was first created using Onshape e Web and then converted using Ultimaker Cura 5.1.0.

#### 2.2 Parameter

The sample was made using a Creality CR-10 S5 3D printer with a printing volume of XYZ 500 mm, 500 mm, and 500 mm. Printing temperatures of 200°C, 210°C, 220°C, 230°C, and 240°C,

with the fan speed set at 80% and 100% for each printing temperature. The layer thickness, build plate temperature, and printing speed were kept constant, and a single grid infill pattern was utilized.

Table 2. Specimen parameter

Printing temperature (°C)	Fan speed (mm/s)	Temperature bed (°C)	Infill pattern
200, 210, 220, 230, 240	80 and 100	60	grid

### 2.3 Testing and SEM

The testing was conducted using a Carl SEM Type EVO MA10 with a power of 20 kV. The magnifications used were 30x, 100x, and 200x for surface observation, and 9x and 15x for thread observation.

## 3 Results and Discussion

### 3.1 Precision Testing Results

Table 3 presents the measurement results of 3D printing samples at various temperatures immediately after removal from the machine. The data reveals that the precision of the 3D printing process varies depending on the temperature used. Notably, the sample printed at 220°C exhibits the highest deviation compared to the other samples. This is evident in the bolt height deviation, which ranges from 0.16 mm to 0.26 mm, the bolt head diameter deviation of 0.20 mm to 0.30 mm, the bolt shaft diameter deviation of 0.15 mm, and the thickness deviation of up to 0.36 mm. In contrast, the sample printed at 200°C demonstrates the highest precision, with a bolt height deviation of only 0.04 mm to 0.06 mm, a bolt head diameter deviation of 0.1 mm, a bolt shaft diameter deviation of 0.05 mm, and a thickness deviation of 0.16 mm. Consequently, it can be inferred that lower printing temperatures result in higher precision for the produced bolts. However, the same table also indicates that a printing temperature of 240°C yields high precision, with a bolt height deviation of 0.04 mm, a bolt head diameter deviation of 0 mm to 0.1 mm, a bolt shaft diameter deviation of 0.05 mm, and a bolt thickness deviation of 0.04 mm. Furthermore, the measurements suggest that increasing the nozzle speed does not significantly impact the precision of the samples. Thus, it can be concluded that raising the nozzle speed to increase production speed in 3D printing is unlikely to have a substantial effect on dimensional precision quality.

Table 3. Measurements after printing

No. specimen	Printing temperature (°C)	Fan speed (mm/s)	Measurements after printing 40°C (mm)			
			Bolt height	Head diameter	Shaft diameter	Head thickness
B-01	200	80	17.40	12.80	6.30	4.60
B-02		100	17.50	12.80	6.30	4.60
B-03	210	80	17.30	13.10	6.40	4.70
B-04		100	17.30	13.00	6.20	4.50
B-05	220	80	17.30	13.00	6.20	4.40
B-06		100	17.20	12.90	6.20	4.40
B-07	230	80	17.30	13.10	6.30	4.50
B-08		100	17.60	12.70	6.40	4.70
B-09	240	80	17.60	12.70	6.40	4.80
B-10		100	17.60	12.80	6.40	4.80

Tables 4, 5, and 6 present the measurements for 3D printed samples exposed to temperatures of 31°C, 33°C, and 22°C for one hour. Figures 3, 4, and 5 demonstrate that shrinkage occurred in all samples, indicating that PLA+ prototype products will inevitably experience shrinkage [23, 24, 25, 27]. In Fig. 3 (at a

cooling temperature of 31°C), the sample printed at 210°C exhibited the greatest shrinkage, with a 3.125% reduction in bolt shaft diameter. Conversely, the sample printed at the lowest temperature (200°C) showed shrinkage around 1%-1.5% throughout the bolt. Notably, increasing the printing temperature reduced shrinkage, as evidenced in Table 4 for printing temperatures of 220°C, 230°C, and 240°C.

Table 4. Cooling measurements 31°C

No. specimen	Printing temperature (°C)	Fan speed (mm/s)	Measurements 31°C (mm)			
			Bolt height	Head diameter	Shaft diameter	Head thickness
B-01	200	80	17.40	12.60	6.10	4.50
B-02		100	17.30	12.80	6.30	4.50
B-03	210	80	17.20	12.80	6.20	4.50
B-04		100	17.30	12.70	6.20	4.50
B-05	220	80	17.40	12.80	6.30	4.50
B-06		100	17.20	12.90	6.10	4.50
B-07	230	80	17.20	12.70	6.30	4.50
B-08		100	17.60	12.70	6.30	4.70
B-09	240	80	17.60	12.70	6.40	4.80
B-10		100	17.60	12.80	6.40	4.70

Table 5. Cooling measurements 33°C

No. specimen	Printing temperature (°C)	Fan speed (mm/s)	Measurements 33°C (mm)			
			Bolt height	Head diameter	Shaft diameter	Head thickness
B-01	200	80	17.40	12.60	6.20	4.50
B-02		100	17.30	12.80	6.20	4.50
B-03	210	80	17.30	12.70	6.20	4.50
B-04		100	17.20	12.80	6.30	4.50
B-05	220	80	17.40	12.90	6.30	4.50
B-06		100	17.20	12.90	6.20	4.50
B-07	230	80	17.30	12.70	6.40	4.50
B-08		100	17.60	12.70	6.30	4.70
B-09	240	80	17.60	12.70	6.40	4.70
B-10		100	17.60	12.80	6.40	4.80

Table 6. Cooling measurements 22°C

No. specimen	Printing temperature (°C)	Fan speed (mm/s)	Measurements 22°C (mm)			
			Bolt height	Head diameter	Shaft diameter	Head thickness
B-01	200	80	17.40	12.60	6.10	4.50
B-02		100	17.30	12.80	6.20	4.50
B-03	210	80	17.20	12.70	6.20	4.50
B-04		100	17.20	12.80	6.20	4.50
B-05	220	80	17.30	12.90	6.20	4.40
B-06		100	17.10	12.90	6.20	4.40
B-07	230	80	17.20	12.70	6.30	4.50
B-08		100	17.50	12.70	6.30	4.60
B-09	240	80	17.50	12.70	6.40	4.60
B-10		100	17.50	12.80	6.40	4.70

A similar trend was observed in Fig. 4 and Fig. 5, where the most significant shrinkage in bolt thickness occurred at 210°C, reaching 4.125% and 4.255% at environments of 33°C and 22°C, respectively. Conversely, the sample produced at 200°C exhibited shrinkage of 0%-2.174% in both 33°C and 22°C environments. Increasing the printing temperature generally resulted in reduced shrinkage across all parts, except for the bolt thickness in the sample printed at 240°C. Fig. 4 demonstrated shrinkage of

2.083%, while Fig. 5 exhibited shrinkage ranging from 2.083% to 4.175%. This can be attributed to higher printing temperatures rendering the filament more fluid, enabling it to fill empty spaces more effectively. The absence of empty spaces contributes to more stable particles that retain their positions during cooling or storage.

Figures 2, 3, 4, and 5 portray the measurement results graphically for recently completed samples stored at 31°C, 33°C, and 22°C. It is important to note that these graphs differ from the data presented in Tables 4, 5, and 6. The tables provide the measurement scales used to compare with the measurements in Table 3, clearly displaying the shrinkage of each sample. The graphs in Figures 2, 3, 4, and 5, on the other hand, compare the measurements against the design dimensions specified in Table 1 and Fig. 1. The depicted data indicates that deviations differ across each part of the bolt-shaped sample. For example, the bolt height demonstrates the greatest deviation in samples printed at temperatures between 210°C and 230°C, ranging from 0.916% to 1.489% in environments of 31°C and 33°C, and 0.916% to 2.062% in a 22°C storage environment. However, for printing temperatures of 200°C and 240°C, the size deviation remains below 1% under all storage conditions.

As for the bolt head diameter, the deviation reaches 1.57% at a printing temperature of 220°C, while the deviation in other samples remains below 1%. The bolt shaft diameter experiences decreasing deviation as the printing temperature increases. Calculations reveal a deviation of 3.937% for the sample printed at 200°C, decreasing to 2.362% at 210°C and 220°C, and reaching 0.787% (less than 1%) at 240°C. This trend remains consistent for all storage conditions at 31°C, 33°C, and 22°C. The bolt width follows a similar pattern, with the largest deviation observed in the sample printed at 200°C, reaching 5.462%, and the smallest deviation in the sample printed at 240°C, at 1.261%. These results suggest that higher printing temperatures lead to smaller deviations.

Moreover, it is evident that dimensions related to width exhibit deviations exceeding 2% and even 5%, while measurements related to height demonstrate deviations around 1%. This indicates a higher likelihood of deviations occurring in dimensions associated with width (horizontal measurements). FDM, a printing method that involves stacking one filament on top of another until the entire part is printed [20, 21], likely contributes to these observed deviations. As the bottom layer is secured by the workpiece, particles tend to shift left or right just before solidifying. This shifting phenomenon is likely the cause of the observed deviations.

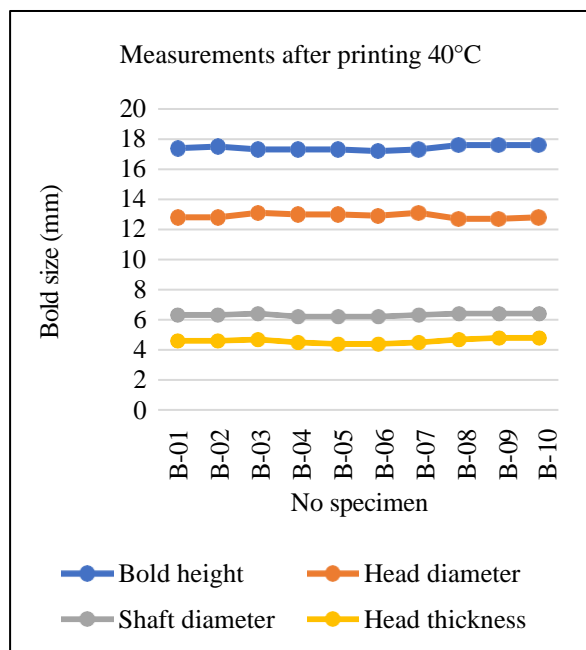


Fig. 2. Graph of specimen measurements after printing.

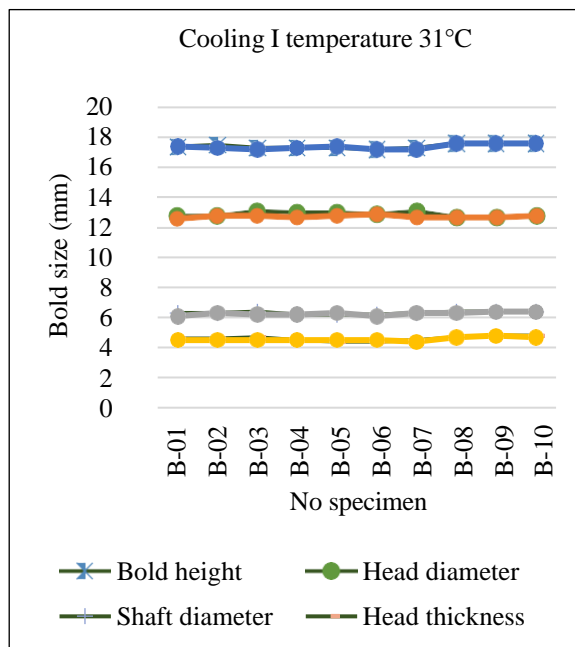


Fig. 3. Cooling graph of specimens at 31°C.

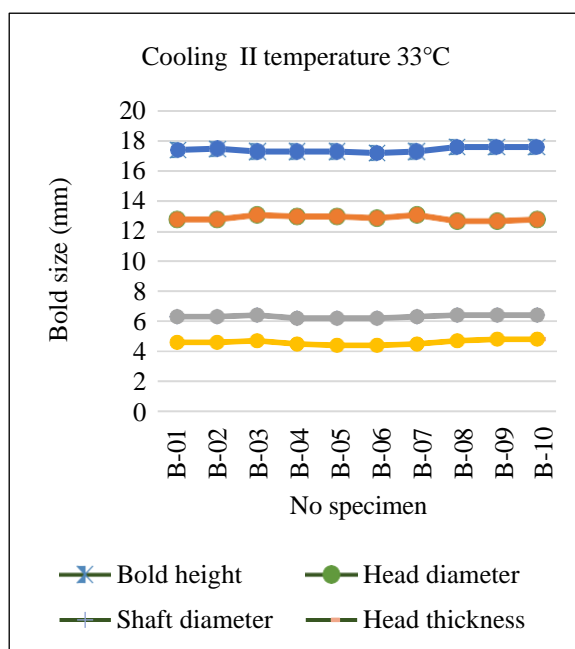


Fig. 4. Cooling graph of specimens at 33°C.

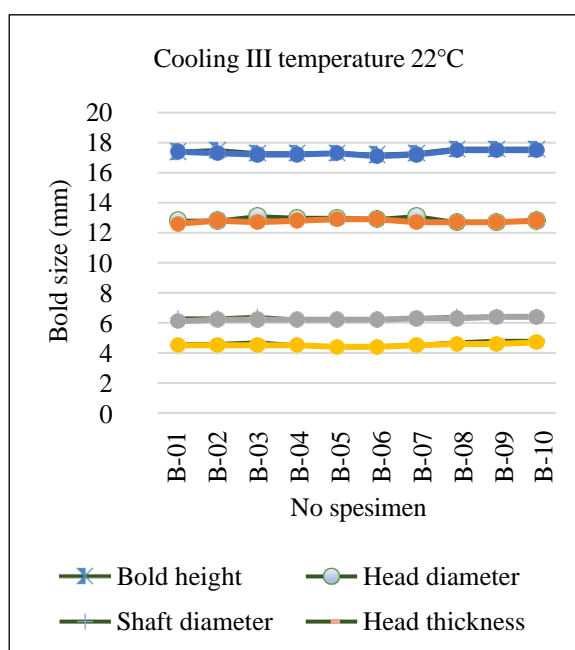


Fig. 5. Cooling graph of specimens at 22°C.

### 3.2 Scanning Electron Microscope (SEM) Testing

Scanning Electron Microscope (SEM) testing is used to observe the microstructure and roughness of the specimen. Based on the heating and cooling tests conducted, the next step is to

examine the microstructure [26] of each specimen, based on the results obtained at printing temperatures of 200°C, 210°C, 220°C, 230°C, and 240°C with a fan speed of 100 mm/s. Fig. 6-Fig. 10 are the SEM test results for each specimen.

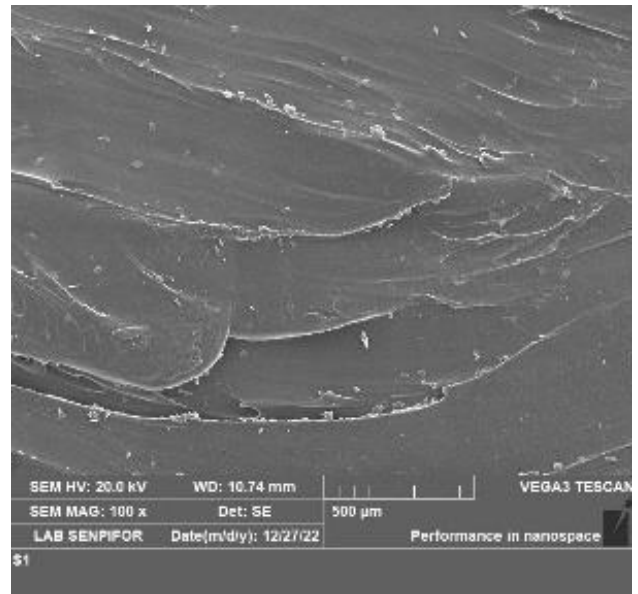
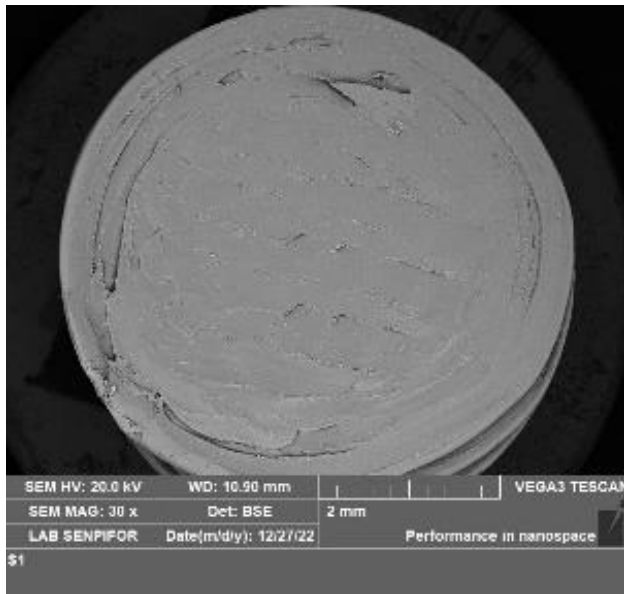


Fig. 6. SEM results of microstructure for specimen B-02 at 100x magnification.

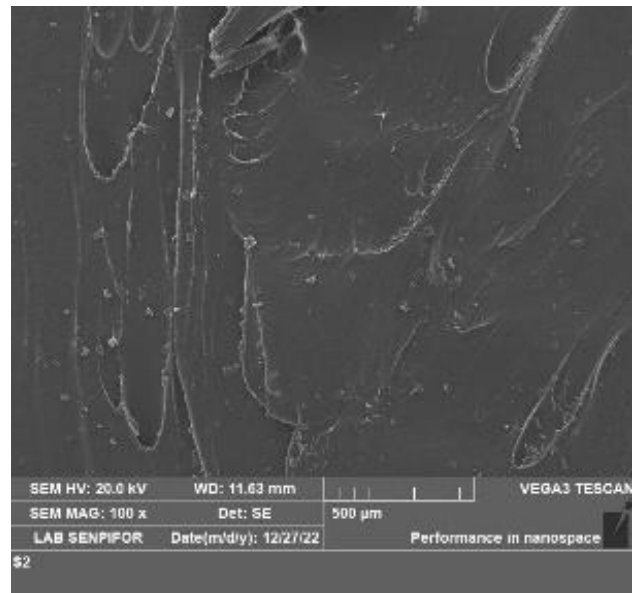
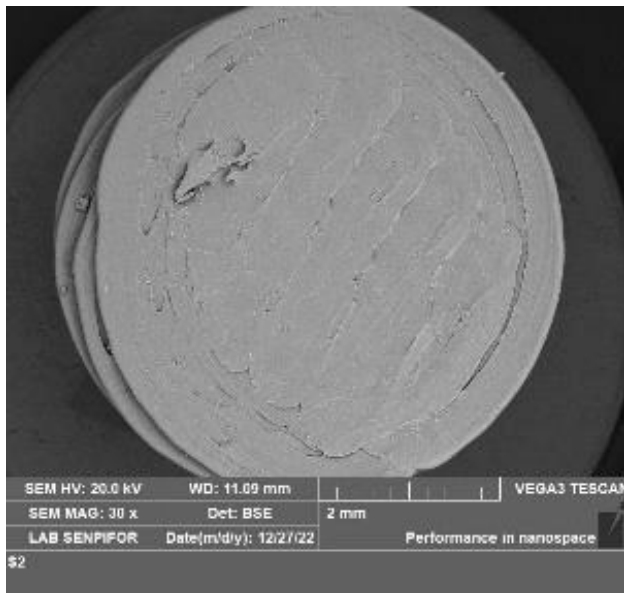


Fig. 7. SEM results of microstructure for specimen B-04 at 100x magnification.

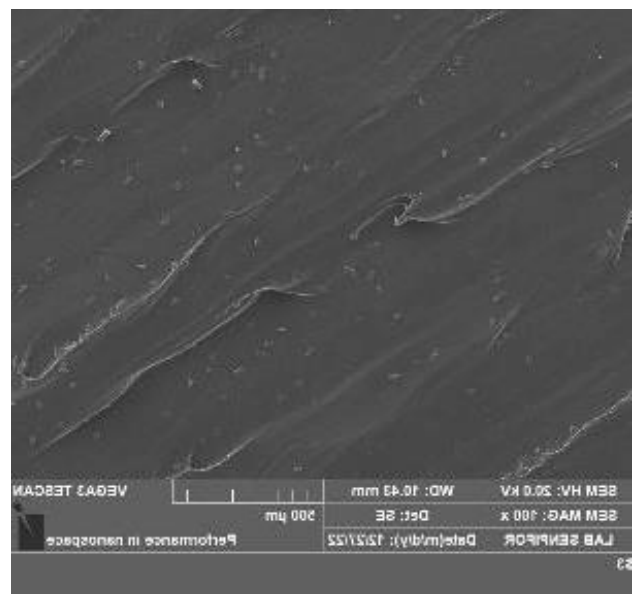
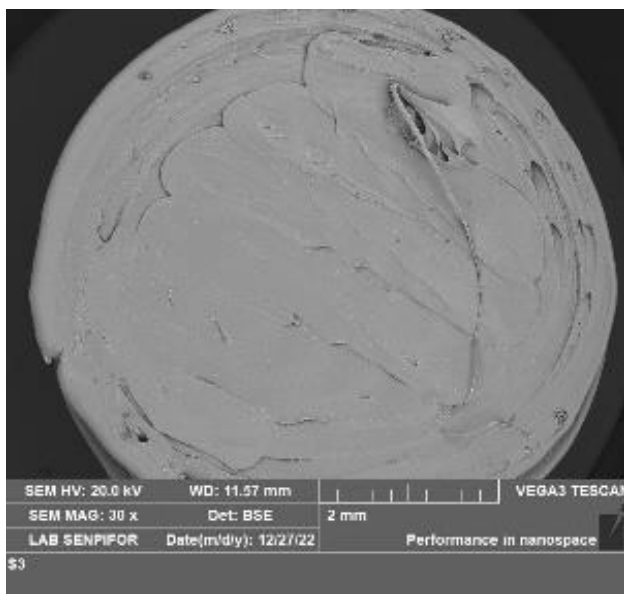


Fig. 8. SEM results of microstructure for specimen B-06 at 100x magnification.

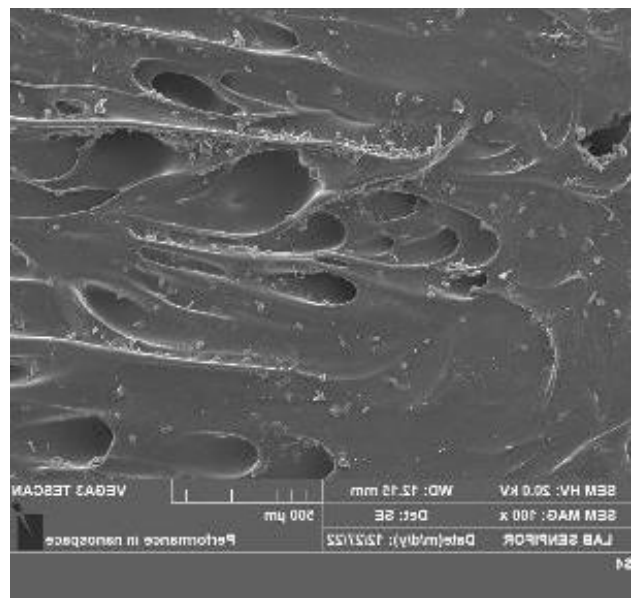
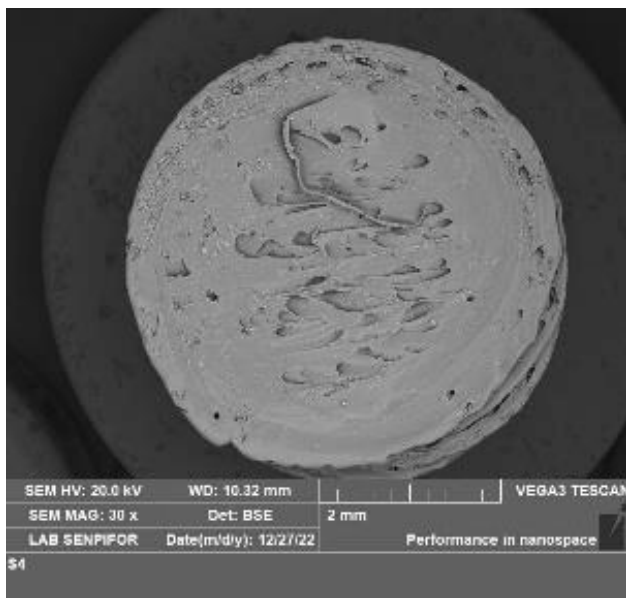


Fig. 9. SEM results of microstructure for specimen B-08 at 100x magnification.

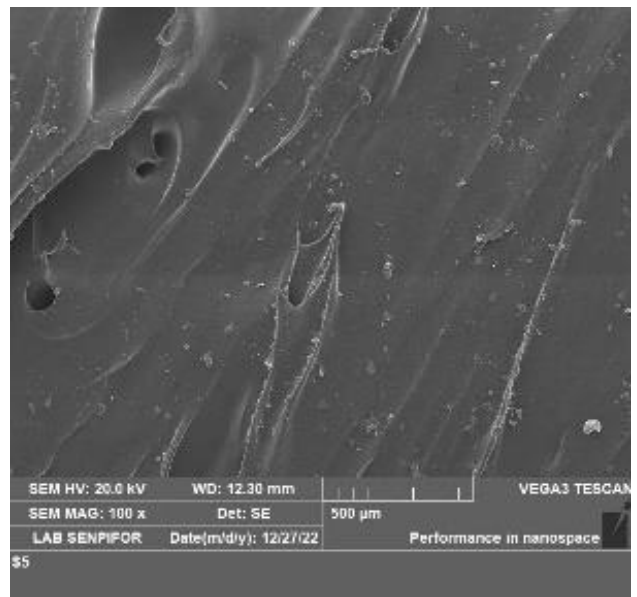


Fig. 10. SEM results of microstructure for specimen B-10 at 100x magnification.

Fig. 6 through 10 are images of the bolt head surface taken by SEM. The four images above show similar features. At 30x magnification, we can see that each image has circular shapes that appear to be stacked on top of each other. This is also observed when 100x magnification is applied. The amorphous structure of each specimen, which is characteristic of plastic structures, is shown in the images. Therefore, surface observation of 3D-printed

results is not highly recommended since there are not many significant differences.

Meanwhile, Fig. 11 and Fig. 12 display the SEM observations for each sample at printing temperatures ranging from 200°C to 240°C. It is worth noting that the magnification was adjusted in order to obtain specific information.

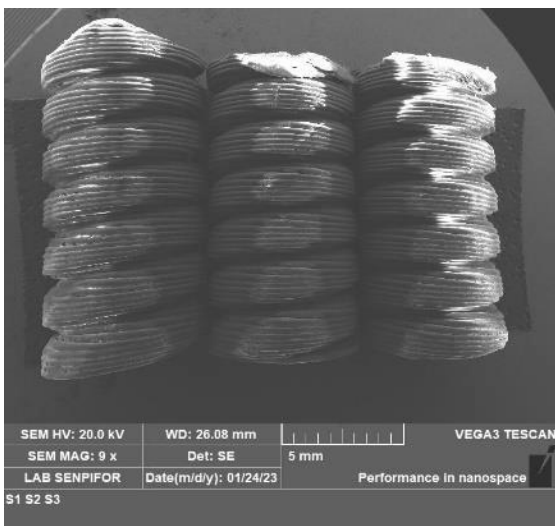


Fig. 11. SEM results on the threads of bolts B-02, B-04, and B-06.

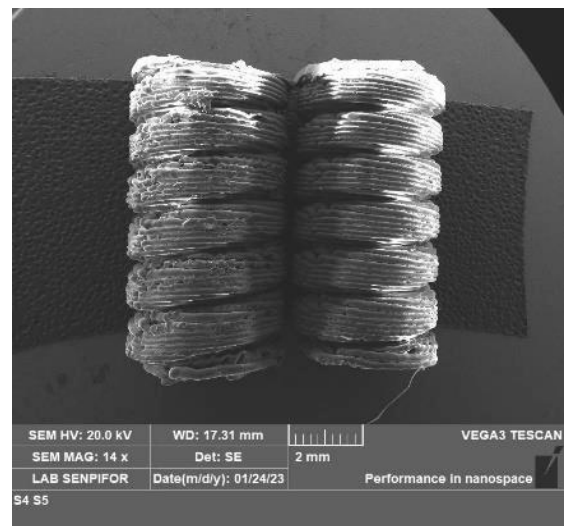


Fig. 12. SEM results on the threads of bolts B-08 and B-10.

Fig. 12 reveals a minimal presence of fibers on the bolt shaft, in contrast to Fig. 13, which illustrates a different scenario for samples printed at temperatures of 230°C and 240°C. In this case, obstructive fibers are detectable, potentially causing friction on the bolt threads when the bolt is subsequently fitted onto a ring or another component. For objects with straightforward requirements, such as a smooth horizontal or vertical surface, minor smoothing can be achieved through machining processes like grinding or milling. However, for objects with intricate shapes, particularly those with fits like bolts, such processes can complicate installation. Therefore, this matter should be taken into consideration during the 3D printing process. It is important to note that higher printing temperatures tend to result in rough fibers on the printed object.

#### 4 Conclusion

1. The shrinkage of 3D-printed objects decreases with increasing printing temperature. However, even at a printing temperature of 240°C, the shrinkage value remains nearly the same as at the lowest printing temperature of 200°C, with deviations in bolt height of 0.14 mm, bolt head diameter of 0-0.1 mm, bolt shaft diameter of 0.05 mm, and bolt thickness of 0.04 mm.
2. The deviation of 3D-printed results from the design dimensions decreases as the printing temperature increases. This is evident from the highest deviation occurring in the bolt shaft diameter, which reaches 5.24%, whereas the deviation in the 240°C printing sample is only 1.261%.
3. Surface observation of bolts using SEM is not recommended as it does not reveal significant differences, and the images tend to appear similar.
4. SEM cross-sectional observations of the bolt shaft indicate that 3D-printed samples with higher printing temperatures tend to exhibit more fibers (hairs) compared to samples produced at lower printing temperatures. These fibers can potentially cause friction when in contact with other objects.

#### References

- [1] P. Pristiansyah, H. Hasdiansah, and S. Sugiyarto, "Optimasi Parameter Proses 3D Printing FDM Terhadap Akurasi Dimensi Menggunakan Filament Eflex," *Manutech: Jurnal Teknologi Manufaktur*, vol. 11, no. 01, pp. 33–40, 2019.
- [2] M. D. A. Athallah, S. Sugiyanto, and R. Ismail, "PENGARUH TEMPERATUR NOZZLE 3D PRINT TERHADAP FLEXURAL STRENGTH BIODKOMPOSIT BERBAHAN PLA, PCL, DAN HIDROKSIAPATIT DARI CANGKANG RAJUNGAN," *JURNAL TEKNIK MESIN*, vol. 10, no. 2, pp. 249–254, 2022.
- [3] K. Kunarto and A. A. Pratama, "ANALISA TEMPERATUR PADA HEATER NOZZLE DENGAN VARIASI NOZZLE TERHADAP HASIL PRODUK PRINTER 3D MENGGUNAKAN FILAMENT PLA," *JURNAL TEKNIK MESIN*, vol. 9, no. 1, 2021.
- [4] B. A. Setyawan and Y. Ngadiyono, "Analisis Pengaruh Tingkat Kelembaban Filamen PLA Terhadap Nilai Kekuatan Mekanik Hasil Cetak 3D Printing," *Jurnal Dinamika Vokasional Teknik Mesin*, vol. 7, no. 1, pp. 1–11, 2022.
- [5] Z. S. Suzen and H. Hasdiansah, "Pengaruh Geometri Infill terhadap Kekuatan Tarik Spesimen Uji Tarik ASTM D638 Type IV Menggunakan Filamen PLA+ Sugoi," *Jurnal Rekayasa Mesin*, vol. 16, no. 2, pp. 140–147, 2021.
- [6] K. S. Putra and U. R. Sari, "Pemanfaatan teknologi 3d printing dalam proses desain produk gaya hidup," in *Seminar Nasional Sistem Informasi dan Teknologi Informasi*, 2018, pp. 917–922.
- [7] M. Fakultas, T. Oleh, and F. Farikhin, "Analisa Scanning Electron Microscope Komposit Polyester Dengan Filler Karbon dan Karbon Non Aktif." 2016
- [8] S. Cahyati and A. Marpaung, "Pengaruh kecepatan kipas pendingin pada mesin 3D printing terhadap kualitas produk cetak," *Jurnal Rekayasa Mesin*, vol. 17, no. 3, 2022.
- [9] F. T. Cetio, "Pengaruh Proses Annealing dan Printing Speed 3D Printed Fused Deposition Modelling Terhadap Kekuatan Tarik Pada Hasil Cetak Berbahan Polylactic Acid (PLA)," 2023.
- [10] J. Triyono, H. Sukanto, R. M. Saputra, and D. F. Smaradhana, "The effect of nozzle hole diameter of 3D printing on porosity and tensile strength parts using polylactic acid material," *Open Engineering*, Published by De Gruyter Open Access, Aug. 12, 2020.
- [11] S. Islam, G. Bhat, and P. Sikdar. "Thermal and acoustic performance evaluation of 3D-printable PLA materials." *Journal of Building Engineering*, vol. 67, 15 May 2023, pp. 105979.
- [12] S. Saefudin, D. Cahyandari, I. Y. Afif, S. Raharjo, M. Subri, and A. N. Anwar. "Peningkatan Sifat Mekanik Produk 3D Printing dengan Proses Annealing." *Jurnal Teknik Industri*, vol. 19, no. 1, April 2023, hal. 73-80.
- [13] H. A. Pamasaria, Herianto, and T. H. Saputra. "Pengaruh Parameter Proses 3D Printing Tipe FDM (Fused Deposition Modeling) Terhadap Kualitas Hasil Produk." *Seminar Nasional IENACO*, 2019.
- [14] E. Pratama, A. I. Alamsyah, and R. S. Prasetyo. "Pengaruh Suhu Ekstrusi Terhadap Densitas dan Laju Degradasi pada Filamen 3D Print Berbahan PLA, PCL, dan HA." *Jurnal Teknik Mesin*, vol. 19, no. 1, 2022.
- [15] W. H. Pratama, Hasdiansah, and Husman. "Optimasi Parameter Proses 3D Printing Terhadap Kuat Tarik Material Filamen PLA + Menggunakan Metode Taguchi." *SJOME (Scientific Journal of Mechanical Engineering)*, vol. 3, no. 1, Agustus 2021, hal. 1-10.
- [16] K. Selo Ageng, I. R. Putra, and Sehonon "Pengembangan Material Komposit Tahan Panas dengan Menggunakan Metode 3D Printing dan Hand Lay Up." *STTKD: Jurnal Teknik, Elektronik, dan Engine*, vol. 9, no. 1, Juli 2023, hal. 23-34.
- [17] M. Saleh, S. Anwar, A. Y. AlFaify, A. M. Al-Ahmari, and A. E. E. Abd Elgawad. "Development of PLA/recycled-desized carbon fiber composites for 3D printing: Thermal, mechanical, and morphological analyses." *Journal of Materials Research and Technology*, vol. 29, March–April 2024, pages 2768-2780.
- [18] R. Avriansah, Erwanto, and Pristiansyah. "Optimasi Parameter Proses 3D Printing Terhadap Kekuatan Tarik Filament Polyethylene Terephthalate Glycol." *Prosiding Seminar Nasional Inovasi Teknologi Terapan*, 2022, hal. 45-56.
- [19] P. B. Frandika. "Pengaruh Infill Geometry, Printing Speed, dan Nozzle Temperature Terhadap Kekuatan Impak Menggunakan Filamen ST PLA." *Jurnal Teknik dan Material*, 2021.
- [20] R. Fadhlurrohman. "Studi Numerik Heat Sink Model Mosquito Hotend pada FDM 3D Printer untuk Mengetahui Karakteristik Perpindahan Panas." *Jurnal Teknik Mesin dan Energi*, 2023.
- [21] R. Muhammad. "Pengaruh Proses Annealing dan Building Orientation pada 3D Printed Fused Deposition Modelling (FDM) Terhadap Kekuatan Tarik pada Hasil Cetak Berbahan Polylactic Acid (PLA+)." *Jurnal Teknik Material*, 2024.
- [22] M. A. Satrio. "Pengaruh Suhu Post Curing Terhadap Kekuatan Bending Komposit Sandwich Menggunakan Core 3D Printing Pola Square." *Jurnal Teknik dan Material*, 2023.
- [23] F. D. Mahesa, D. Budiman, M. Mulyadi, R. Rakiman, Y. Yuliarman, and A. Zamri. "Pengaruh Pola Kerapatan Infill Pattern Terhadap Kekuatan Tarik Filamen PLA 3D Printer." *PROTEMAN: Professional Technology and Manufacturing*,

vol. 1, no. 1, 2024, hal. 05–09.

- [24] A. Setiawan. “Pengaruh Parameter Proses Ekstrusi 3D Printer Terhadap Sifat Mekanis Cetak Komponen Berbahan Filament PLA (Poly Lactic Acid).” *Jurnal Teknik STTKD*, vol. 4, no. 2, Desember 2017.
- [25] N. Amalia, F. Habib, and M. Balfas. “Pengaruh Infill Angle pada Proses 3D Printing FDM Terhadap Tensile Strength Material PLA+.” *Jurnal Teknologi dan Material*, vol. 2, no. 2, 2022.
- [26] M. Tajima, S. Fujimoto, Y. Honda, and Y. Matsumoto. “Selective electron beam melting additive manufacturing of inconel 718 with varied process parameters: The effects on microstructure and mechanical properties.” *Journal of Manufacturing Processes*, vol. 89, 2024, hal. 21-29.
- [27] H. Bakhtiari, A. Nouri, and M. Tolouei-Rad. “Impact of 3D printing parameters on static and fatigue properties of polylactic acid (PLA) bone scaffolds.” *International Journal of Fatigue*, vol. 186, 2024.